Electron induced *pd* and *ppn* breakup of ^{3}He with full inclusion of final-state interactions

J. Golak,[2] H. Kamada,[1] H. Witała,[2] W. Glöckle,[1] and S. Ishikawa[3]
[1]*Institut für Theoretische Physik II, Ruhr-Universität Bochum, D44780 Bochum, Germany*
[2]*Institute of Physics, Jagellonian University, PL-30059 Cracow, Poland*
[3]*Department of Physics, Tohoku University, Sendai 980, Japan*
(Received 15 June 1994)

Exclusive electron scattering on ^{3}He leading to the *pd* and *ppn* breakup is studied under full treatment of the final-state interaction (FSI). Realistic NN forces are used. The importance of FSI is demonstrated in several examples, among them deuteron knock-out data which are well described.

PACS number(s): 21.45.+v, 25.30.Fj, 21.30.+y

I. INTRODUCTION

With the new high-duty cycle electron accelerators coming up, coincidence experiments between the scattered electron and nucleons resulting from the breakup of a nuclear target will become feasible. Due to the larger number of structure functions and their dependence on more momentum variables one can expect to get more information from those exclusive processes than from purely inclusive or even elastic processes. It should however be guaranteed that the final-state interaction (FSI) is well under control in order to be sure to unambiguously locate the effects one would like to study, like meson-exchange current (MEC), electromagnetic hadronic form factors or properties of the target wave function. This is possible in the deuteron and as we will show also in the $A = 3$ system using realistic NN forces.

Already quite some time ago the importance of treating the final-state interaction between the three final nucleons and the consistency between the three-nucleon bound state and the three-nucleon scattering state has been recognized. At that time, however, due to the lack of computational power, the forces were quite simple, low rank separable ones. The very first electrodisintegration calculations of ^{3}He and ^{3}H were performed in [1], where the ground state was solved by the Faddeev method, in the final state however the interaction was kept only within the spectator pair (the two nucleons, which have not absorbed the photon under single nucleon current assumption). Very similar in nature and techniques is of course the photodisintegration, where the first Faddeev calculations for the $3N$ continuum [2] appeared and where the importance of the rescattering with the spectator nucleons was emphasized. One step further was the work in [3], where for the two- and three-body photodisintegrations of ^{3}He (^{3}H) both ground state and $3N$ continuum were treated consistently as solutions of the same $3N$ Hamiltonian. This exact treatment, though still with simple NN forces, already allowed to ask detailed questions [4] like the suppression of the isospin $T = \frac{1}{2}$ in three-body photodisintegration of ^{3}He. Then the first calculation for two-body electrodisintegration of ^{3}He (^{3}H) came up in [5]. Although also the formalism for three-body disintegration in the context of separable forces was formulated, limitations of computer resources prevented their realization. It then took quite some time that the three-body electrodisintegration has been treated in [6], now using simple *s*-wave local forces in an unitary pole expansion (UPE) or only unitary pole approximation (UPA) form. The conclusion again was that a proper description has to take into account contributions from the complete multiple scattering series, which strongly underlines the importance of FSI. Due to the lack of kinematically complete *ppn* breakup data that calculation was applied to a set of existing inclusive data, where the two-body and three-body electrodisintegration processes are both involved.

Physically and formally closely related are *pd* radiative capture processes, where a first configuration space $3N$ calculation based on solutions of the Faddeev equation for the $3N$ bound state and $3N$ scattering states appeared [7] using the Reid NN force. Thereby as in the following studies [8,9] the interest was in the sensitivity of tensor analysing powers to properties of the $3N$ bound state and to the NN forces. The treatment of the initial-state interaction turned out to be very crucial and also the inclusion of higher NN force components. In [8] realistic NN forces and even $3N$ forces have been used in a consistent $3N$ Faddeev treatment for both bound state and continuum states. In [9] separable forces were employed but also an EST (Ernst-Shakin-Thaler) expansion form of the Paris potential.

At very low energies *nd* capture has also been treated [10] using a configuration space Faddeev method and realistic $2N$ and $3N$ forces. The method of correlated orthogonal states [11] represents the continuum to some extent and puts in short-range correlations. Although the states are not proper solutions of the $3N$ Hamiltonian their use in studying inclusive response functions clearly showed significant improvement over plane-wave impulse approximation (PWIA) results and underlined the importance of treating the correlations between the three nucleons in the final state as consequently as in the $3N$ bound state.

A recent development is the Euclidean response method [12] applied to inclusive responses. By path integral techniques one calculates the Laplace transform of the response functions and compares them to the cor-

responding Laplace transformed data. This is an exact method and includes the full dynamics of the chosen Hamiltonian. Related to that are first trials with Stieltjes transforms [13] or transformations by a Lorentz kernel [14].

In this paper we extend our first study [15] on the *pd* electrodisintegration of ^{3}He to the full *ppn* breakup of ^{3}He using realistic NN forces with full inclusion of all rescattering processes. To the best of our knowledge this is the first time that this could be realized. Also in relation to [15] we succeeded now to include all relevant NN force components, while in [15] we restricted ourselves to the states $^1S_0$ and $^3S_1$-$^3D_1$. This has significant importance in certain observables. The progress in relation to [6] is that we use realistic NN forces with all their complexities, which is clearly needed for a good description of most data, not of all however. For instance, the longitudinal response in inclusive scattering can fairly well be described by simple pure s-wave forces, like the one used in [6]. Trivially spin observables are the other extremes where pure s-wave forces would fail totally. Also in relation to the older work in the seventies and sixties the use of realistic forces is a decisive step forward. These forces are linked to field theoretical ingredients, whereas the *ad hoc* chosen ansätze have no such connection. This paper provides the technical tools to handle any sort of NN forces, which certainly will be of great importance in the years to come, where new concepts will enter into the expressions of nuclear forces.

In relation to [6] there is also a formal step forward. In [6] the final scattering state for the *ppn* breakup is worked out separately and one faces the technical difficulties of rescattering singularities of second order in the two-nucleon t matrix for the 3 to 3 scattering amplitude. This can be totally avoided by rewriting the nuclear matrix element for *ppn* breakup and applying the rescattering operations to the initial $3N$ bound state together with the current operator. In this matter *pd* as well as *ppn* breakup can be treated on the same footing and no additional technical problems arise by going from the two-body to the three-body breakup. Short descriptions have already been given in [16,17]. We stick to the notation introduced in [18], where elastic electron scattering on ^{3}He has been treated and more heavily on the notations used in [15]. Thus the description of the formalism in Sec. II can be rather brief, with the exception of the way we incorporate the *ppn* breakup.

In Sec. III we supplement the results for *pd* breakup already given in [15] by emphasizing the necessity for choosing realistic NN forces and including higher partial wave force components. As an application we compare our results to some data taken at NIKHEF. We strongly feel that there should be more data on the *pd* breakup covering the whole angular distribution of the ejected proton (deuteron) (and not just a few angles, as exist up to now). Especially interesting would be to map out the deuteron knockout peak, since there rescattering processes under the action of realistic forces are very important. This would shed light on the issue, whether that deuteron knockout peak area can be used as a tool to "see" *np* correlations in the target.

For the full breakup there exist up to now no data in so-called complete kinematics. Thus we show just some examples illustrating interesting structures and the need of a correct control of FSI. More extended studies are in preparation, especially the search for breakup configurations, where FSI is negligible and therefore dynamical properties of the initial $3N$ bound state and of the current operator can be more clearly seen. Trivially, a prerequisite to do that is, that one can control FSI for the full breakup of ^{3}He and this is one of the messages of this paper.

There are data, however, on inclusive scattering, where three-body breakup contributes. Unfortunately, the theoretical analysis of these data requires extensive numerical calculations, since for every energy transfer of the photon the Faddeev equations have to be solved. The necessary numerical resources are not available to us in a short time. We are working on that analysis of the inclusive data and shall report on it in a forthcoming paper.

A brief summary and outlook is given in Sec. IV.

II. FORMALISM

The derivation of the exclusive inelastic scattering cross section can be carried through along the lines displayed, for instance, by de Forest [19]. We refer to [15,18] for details of our notation and just quote the result for the eightfold differential unpolarized *ppn* breakup cross section

$$\frac{d^8\sigma}{d\hat{k}'dk'_0d\hat{p}_1d\hat{p}_2dE_1} = \sigma_{\rm Mott}(v_CW_C + v_TW_T + v_IW_I + v_SW_S + v_XW_X + v_YW_Y)\rho_{3N} \ . \tag{1}$$

The momentum of the scattered electron is $k' = (k'_0, \vec{k}')$, the directions of the two nucleons detected in addition to the electron are denoted by $\hat{p}_1$ and $\hat{p}_2$, respectively, and the nucleon kinetic energies by E_i. Aside from the Mott cross section and the phase-space factor given below we see six structure functions W going together with kinematical factors v. It has been shown quite generally that for heavier targets and further fragmentations the number six is not surpassed [20]. The first four terms have well-known analytical forms, as displayed in our notation in [15], and the last two are

$$W_X = \tfrac{1}{2}\sum 2\,{\rm Re}(N_0N^*_\perp) \ , \tag{2}$$

$$W_Y = \tfrac{1}{2}\sum(-2){\rm Re}(N_\parallel N^*_\perp) \ , \tag{3}$$

$$v_X = -\frac{Q^2}{\vec{Q}^2}\left(-\frac{Q^2}{\vec{Q}^2} + \tan^2\frac{\theta_e}{2}\right)^{1/2}\sin\phi \ , \tag{4}$$

$$v_Y = -\frac{Q^2}{\vec{Q}^2}\cos\phi\sin\phi \ . \tag{5}$$

The summation in (2) and (3) is over magnetic quantum numbers. The nonrelativistic phase-space factor is

$$\rho_{3N} = \frac{M_N^2 |\vec{p}_1||\vec{p}_2|}{|1 - \frac{\vec{p}_2\vec{p}_3}{|p_2|^2}|} , \tag{6}$$

where $\vec{p}_3 = \vec{Q} - \vec{p}_1 - \vec{p}_2$ and $|\vec{p}_2|$ is determined kinematically.

One avoids kinematical singularities by representing the breakup cross section along the kinematically allowed locus in the $E_2 - E_1$ plane and measured by the arclength S along that locus (on which all events have to lie). Then

$$\rho_{3N} = \frac{M_N^2 |\vec{p}_1||\vec{p}_2|}{(|1 - \frac{\vec{p}_2\vec{p}_3}{|\vec{p}_2|^2}|^2 + |1 - \frac{\vec{p}_1\vec{p}_3}{|\vec{p}_1|^2}|^2)^{1/2}} \frac{dS}{dE_1} . \tag{7}$$

This is a well known and usual device in the treatment of nd breakup [21].

Now to the central quantity, the nuclear matrix element

$$N^\mu \equiv \langle \Psi^{(-)}_{\text{scatt}} \vec{P}' | \hat{j}^\mu | \Psi_{\text{bound}} \hat{P} \rangle . \tag{8}$$

Here $\Psi^{(-)}_{\text{scatt}}$ and Ψ_{bound} are fully antisymmetric scattering and bound-state solutions of the $3N$ Schrödinger equation, respectively, and $\hat{j}_\mu$ the hadronic current operator, which in this paper is taken to be composed of single nucleon contributions only. In the laboratory system $\vec{P} = 0$ and the total final nuclear momentum is $\vec{P}' = \vec{Q}$, the photon momentum. Then analogously to pd breakup described in [15] we can write for the full breakup

$$N^\mu = 3\langle \Psi^{(-)}_{\vec{p}\vec{q}} m_1, m_2, m_3 | j^\mu(\vec{Q}) | \Psi_{\text{bound}} m \rangle , \tag{9}$$

where m and $m_1 m_2 m_3$ are magnetic spin quantum numbers of the initial and final states, $\vec{p}$ and $\vec{q}$ standard Jacobi momenta [22] describing the asymptotic relative motion of the three outgoing nucleons, and $j^\mu(\vec{Q})$ the current operator for one singled out nucleon as given in [15].

We shall now show that the full breakup process can be handled in the same manner as the pd breakup, not requiring care as in [6]. In fact both processes can be calculated in one shot, just using different quadratures at the end.

The final scattering state is Faddeev decomposed

$$\Psi^{(-)} = (1 + P_{12}P_{23} + P_{13}P_{23})\psi \equiv (1 + P)\psi , \tag{10}$$

where ψ obeys the Faddeev equation

$$\psi = \phi + G_0^{(-)} t^{(-)} P \psi . \tag{11}$$

Here $G_0^{(-)}$ is the free $3N$ propagator, $t^{(-)}$ the off-shell NN t-operator and ϕ composed of a NN scattering state and a momentum eigenstate of the third nucleon:

$$\phi \equiv \phi^{(-)} = |\vec{p}\rangle_a^{(-)} |\vec{q}\rangle . \tag{12}$$

It is important to note that the two-body scattering state is antisymmetrized as indicated by the subscript a. In case of pd breakup that scattering state is just replaced by the deuteron wave function. For notational simplicity we dropped the magnetic quantum numbers and also the isospin identifications of the nucleons.

Let us now insert (10) and (11) into (9):

$$\begin{aligned} N^\mu = {} & 3\langle \phi | (1 + P) j^\mu(\vec{Q}) | \Psi_{\text{bound}} \rangle \\ & + 3\langle \psi | P t G_0 (1 + P) j^\mu(\vec{Q}) | \Psi_{\text{bound}} \rangle . \end{aligned} \tag{13}$$

In the first term we separate the part with no interaction in the final state:

$$N^{\mu,3N}_{\text{PWIAS}} \equiv 3\langle \phi_0 | (1 + P) j^\mu(\vec{Q}) | \Psi_{\text{bound}} \rangle , \tag{14}$$

where

$$|\phi_0\rangle = |\vec{p}\rangle_a |\vec{q}\rangle . \tag{15}$$

Then let us look into all rescattering processes:

$$\begin{aligned} N^{\mu,3N}_{\text{rescatt}} \equiv {} & 3\langle \phi_0 | t G_0 (1 + P) j^\mu(\vec{Q}) | \Psi_{\text{bound}} \rangle \\ & + 3\langle \psi | P t G_0 (1 + P) j^\mu(\vec{Q}) | \Psi_{\text{bound}} \rangle . \end{aligned} \tag{16}$$

Its physical content can be nicely displayed by iterating (11), which leads to the multiple rescattering series

$$\begin{aligned} N^{\mu,3N}_{\text{rescatt}} \equiv {} & 3\langle \phi_0 | t G_0 (1 + P) j^\mu(\vec{Q}) | \Psi_{\text{bound}} \rangle \\ & + 3\langle \phi_0 | (1 + t G_0) P t G_0 (1 + P) j^\mu(\vec{Q}) | \Psi_{\text{bound}} \rangle \\ & + 3\langle \phi_0 | (1 + t G_0)(P t G_0)(P t G_0)(1 + P) j^\mu(\vec{Q}) | \Psi_{\text{bound}} \rangle + \cdots \end{aligned} \tag{17}$$

$$\begin{aligned} = {} & 3\langle \phi_0 | (1 + P) t G_0 (1 + P) j^\mu(\vec{Q}) | \Psi_{\text{bound}} \rangle \\ & + 3\langle \phi_0 | (1 + P)(t G_0 P) t G_0 (1 + P) j^\mu(\vec{Q}) | \Psi_{\text{bound}} \rangle \\ & + 3\langle \phi_0 | (1 + P)(t G_0 P)(t G_0 P) t G_0 (1 + P) j^\mu(\vec{Q}) | \Psi_{\text{bound}} \rangle + \cdots . \end{aligned} \tag{18}$$

We see the various orders of rescattering in the NN t operator, which can easily be visualized in diagrams and at the time we can read off the appropriate Faddeev-like integral equation, which sums up the infinite series:

$$N^{\mu,3N}_{\text{rescatt}} \equiv 3\langle \phi_0 | (1 + P) | U^\mu \rangle \tag{19}$$

with

$$\begin{aligned} |U^\mu\rangle = {} & t G_0 (1 + P) j^\mu(\vec{Q}) | \Psi_{\text{bound}} \rangle \\ & + t G_0 P | U^\mu \rangle . \end{aligned} \tag{20}$$

This is the same integral equation we encountered in the

pd breakup of ^{3}He in [15] in the form of Eq. (37). For *pd* breakup the rescattering matrix element, however, is

$$N^{\mu,pd}_{\rm rescatt} = 3\langle \phi_{pd}|P|U^\mu\rangle \tag{21}$$

thus just a different quadrature (note we changed the normalization of the Faddeev component in Eq. (10) in comparison to [15]) and also we separated a factor 3 from the current operator in [15]. The kernel in (20) is the same we face in the way we treat *nd* scattering [23]. Only the driving term is different.

We solve (20) in a partial wave decomposition and in momentum space, which leads to coupled two-dimensional integral equations. For details we refer to [22,23]. Any type of NN interaction can be used.

III. RESULTS

A. *pd* breakup of ^{3}He

The initial ^{3}He bound state is always based on a 34 channel Faddeev calculation. If not otherwise stated we use the Bonn B NN force [24]. As in [15] we stick to a nonrelativistic treatment including kinematics. Thus the internal energies for the final states are for *pd* breakup

$$T_{pd} = \omega - \frac{\vec{Q}^2}{6M_N} + \epsilon_{^3{\rm He}} - \epsilon_d \ , \tag{22}$$

where $\epsilon_{^3{\rm He}}$ and ϵ_d are the (negative) binding energies of ^{3}He and the deuteron, respectively, and for *ppn* breakup

$$T_{3N} = \omega - \frac{\vec{Q}^2}{6M_N} + \epsilon_{^3{\rm He}} \ . \tag{23}$$

They depend on the energy ω and the momentum $\vec{Q}$ of the virtual photon. For the kinematical conditions used in this paper the deviations from the relativistic forms are smaller than 1%.

In [15] we compared PWIA and its antisymmetrized form, called PWIAS, to the full calculation in case of the *pd* breakup for various $|\vec{Q}|$'s and T_{pd}'s. We found that PWIA was acceptable only in the QFS nucleon knockout area and its quality for a given T_{pd} improved with increasing $|\vec{Q}|$. Here we would like to add a short comment. As shown in Eq. (22) of [15] the single nucleon current operator has the momentum space representation in three-particle space

$$\langle \vec{p}\vec{q}|j^\mu(\vec{Q})|\vec{p}\,'\vec{q}\,'\rangle = \delta(\vec{p}-\vec{p}\,')\delta[\vec{q}\,' - (\vec{q} - \tfrac{2}{3}\vec{Q})]J^\mu(\vec{q},\vec{Q}) \ , \tag{24}$$

where $\vec{p}$ and $\vec{q}$ are standard Jacobi momenta. It is the momentum shift $\vec{q} \to \vec{q}\,' = (\vec{q} - \frac{2}{3}\vec{Q})$ of the nucleon absorbing the virtual photon, which causes the $\vec{Q}$ dependence in the nuclear matrix elements $N^\mu_{\rm PWIAS}$ for PWIAS (see Eq. (33) in [15]) and $\tilde{\tilde{N}}\mu$ containing the remaining complete rescattering process (see Eq. (36) in [15]). In both matrix elements due to the action of that single nucleon current operator the ^{3}He bound state wave function enters as $\Psi_{^3{\rm He}}(\vec{p},\vec{q} - \frac{2}{3}\vec{Q})$. While in PWIA $\vec{q}$ is fixed as $\vec{q}_0[= \frac{2}{3}(\vec{p}_N - \frac{1}{2}\vec{p}_d]$, it is an integration variable for the rescattering term $\tilde{\tilde{N}}_\mu$. In the first case $\vec{q}_0 - \frac{2}{3}\vec{Q}$ is just the missing momentum $\vec{p}_d$ for the proton knockout. If $|\frac{2}{3}\vec{Q}|$ is smaller than $\vec{q}_0$, where T_{pd} fixes $\vec{q}_0$ (see Eq. (39) in [15]), then $\vec{p}_d \neq 0$ and $N^\mu_{\rm PWIAS}$ is smaller than its maximal value reached at $\vec{p}_d = 0$. With increasing $\vec{Q}$, fixed $\vec{q}_0$, and for parallel kinematics ($\vec{q}_0 \parallel \vec{Q}$), one reaches the maximum of $N^\mu_{\rm PWIAS}$ and then it drops monotonously. In the rescattering term it is more complicated. It is obvious from the driving term in (20) or Eq. (37) in [15], the $\vec{q}$ dependence is also present in the kinetic energies of the propagator G_0, which occurs in addition inside t. For large q's, such that the kinetic energy of relative motion $(3/4m)\vec{q}^{\,2}$ is bigger than the available total energy T_{pd}, G_0 and t drop quickly with q. In that case the free propagation is exponentially damped in configuration space. Strong contributions arise, if that kinetic energy is close to T_{pd}. Furthermore also the argument $\vec{q} - \frac{2}{3}\vec{Q}$ is $\Psi_{^3{\rm He}}$ should be small. As an example, for $T_{pd} = 30$ MeV and $|\vec{Q}| = 100$ MeV/c the $|\vec{q}|$ value around $|\frac{2}{3}\vec{Q}|$ fit to T_{pd} and one has strong rescattering, whereas for $|\vec{Q}| = 500$ MeV/c the $|\vec{q}|$ values around $|\frac{2}{3}\vec{Q}|$ suppress G_0 and t and rescattering is much weaker.

While in [15] we restricted the NN force to act in the final state only for $^1S_0$ and $^3S_1$-$^3D_1$, we now include all NN force components for total NN angular momenta up to $j = 2$. The $j = 3$ contributions turned out to be negligible under the kinematical conditions used in this paper.

We display two examples, where we compare calculations using the NN force in the final $3N$ continuum only in the states $^1S_0$ and $^3S_1$-$^3D_1$, up to $j = 1$, and up to $j = 2$. The first example shown in Fig. 1 is for the proton-knockout condition and the data are from [25,26]. We see that the inclusion of the $j = 2$ contribu-

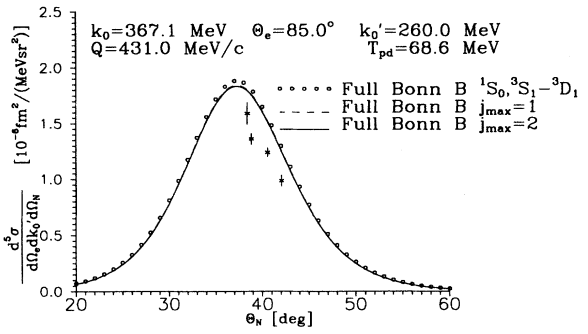

FIG. 1. The quasifree proton knockout peak in *pd* breakup for the T1 configuration of [26]. Rescattering is treated fully and the NN force Bonn B is kept different from zero in the states $^1S_0$, $^3S_1$-$^3D_1$, up to $j_{\rm max} = 1$ and up to $j_{\rm max} = 2$, respectively. θ_N is the proton laboratory angle. The data are from [26].

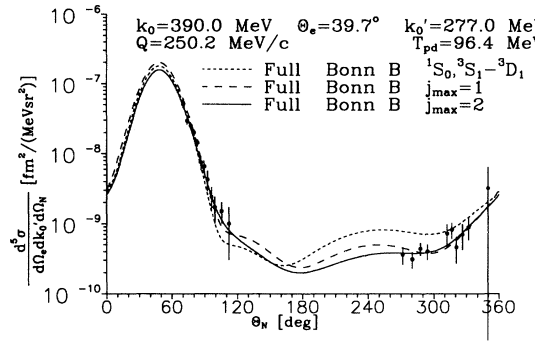

FIG. 2. The full angular proton distribution of *pd* breakup for the HR configuration of [26]. Rescattering is treated fully and the NN force Bonn B is kept different from zero in the states ${}^1S_0$, ${}^3S_1$-${}^3D_1$, up to $j_{\max} = 1$ and up to $j_{\max} = 2$, respectively. The data are from [26].

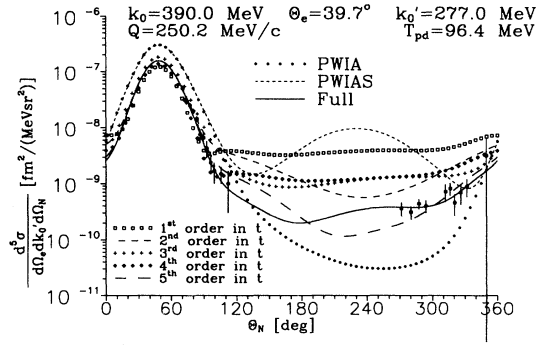

FIG. 4. The HR configuration of [26] for the *pd* breakup. Comparison of PWIA, PWIAS, and partial sums of increasing orders in t. The convergence toward the full solution is very slow.

tions are negligible and the $j = 1$ contributions on top of ${}^3S_1$-${}^3D_1$ lead to changes of only up to 3%. The remaining discrepancy to the data is likely caused by neglecting all relativistic effects (see [15]). In the second example displayed in Fig. 2 the experimental data [26] are more in the slopes and outside of the QFS peak area. Here the $j = 2$ contributions are very significant, up to 19% in the peak area up to 120% around $\theta_n \approx 240°$. In this example the agreement with the data is good.

We would also like to use the kinematics of Fig. 2 to demonstrate again the importance of FSI. As is seen in Fig. 3 neither PWIA nor PWIAS is useful. In the peak area PWIA equals PWIAS and is off by 95% and outside both deviate from the correct treatment by orders of magnitudes. It is also instructive to see the very slow convergence of the multiple scattering series in that example. We display in Fig. 4 the predictions for PWIA, PWIAS, the partial sums of 1st, 2nd,..., order in t for the multiple scattering series and the full solution. It is only in the peak area that the curves are close together. But even there viewed at on a linear scale low order predictions in t are unsatisfactory. Finally this example serves to demonstrate the importance for using realistic NN forces. In Fig. 5 we see that the Bonn B and Paris predictions agree very well among themselves and quite well with the data, whereas MT I-III is totally off (except in the very peak area).

Let us now regard the deuteron knockout peak. There is the expectation [27] that one can learn from that process about np correlations in ^{3}He. Clearly a prerequisite is that FSI is negligible, otherwise one mixes correlations from the $3N$ bound and continuum states. We therefore investigated again under which conditions FSI loses importance. This is illustrated in Figs. 6(a)–6(c). The full treatment of FSI shows the deuteron knockout peak but deviates even at 600 MeV/c strongly from the PWIAS prediction. Therefore, under these conditions an analysis of the deuteron knock-out peak area by PWIAS alone, would lead to inaccurate predictions about ^{3}He properties. This issue deserves further investigation. The case $|\vec{Q}| = 600$ MeV/c also points to the necessity to properly include higher NN force components, here $j = 2$.

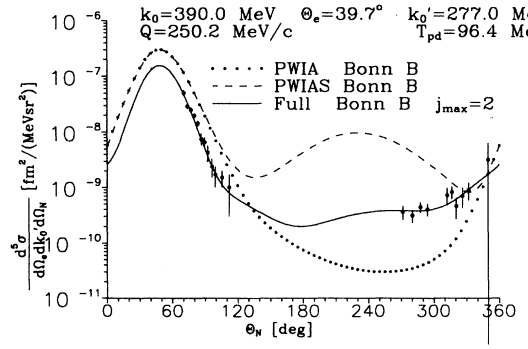

FIG. 3. The full angular proton distribution of *pd* breakup for the HR configuration of [26]. Comparison of PWIA, PWIAS, and the full treatment of rescattering. The Bonn B potential has been kept in the final state up to $j_{\max} = 2$.

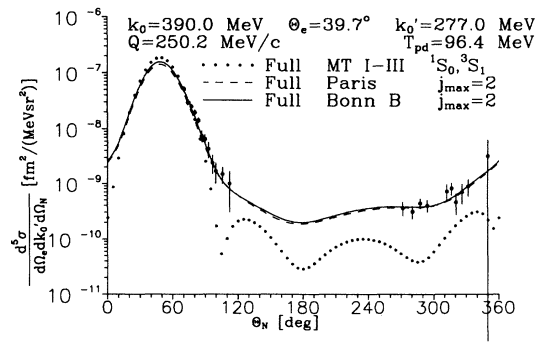

FIG. 5. The HR configuration of [26]. Comparison of Paris and Bonn B predictions to the one based on the MT I-III NN force model.

As is well known, PWIA is totally off in the deuteron knock-out peak area since the photon in the single nucleon current approximation is not hooked to the constituents of the final deuteron. It is the part of PWIAS

$$\frac{1}{\sqrt{3}}\langle\phi_{pd}m_f|Pj^{\mu}_{NR}(\vec{Q})|\phi m\rangle \qquad (25)$$

(see Eq. (33) of [15]), which generates the deuteron knockout, since there the photon is absorbed by the nucleons inside the final deuteron. One may ask, whether that expression (25) is useful to study properties of the ^{3}He wave function, especially, the *np* correlations therein. We shall investigate that question in a forthcoming paper. Here we are satisfied to say that, under the conditions of a single nucleon current operator, the $|\vec{Q}|$'s at which FSI is possibly small, are rather high [see the example of Fig. 6(c)], so that relativistic effects (not included here) might already be appreciable. Therefore strictly spoken, the question of importance or unimportance of FSI has to be investigated again in a relativistic context.

Trivially, in the deuteron knockout peak an oversimplified description of the deuteron itself should not be used. This is demonstrated again for the HR configuration of [26]. Now that cross section is presented in Fig. 7 as function of the deuteron scattering angle. We compare the full Paris and Bonn B predictions ($j_{\max} = 2$) to the one of the pure s-wave force MT I-III. The lack of d-wave admixture in the case of MT I-III, both in the deuteron and the $3N$ scattering process, yields a totally different result.

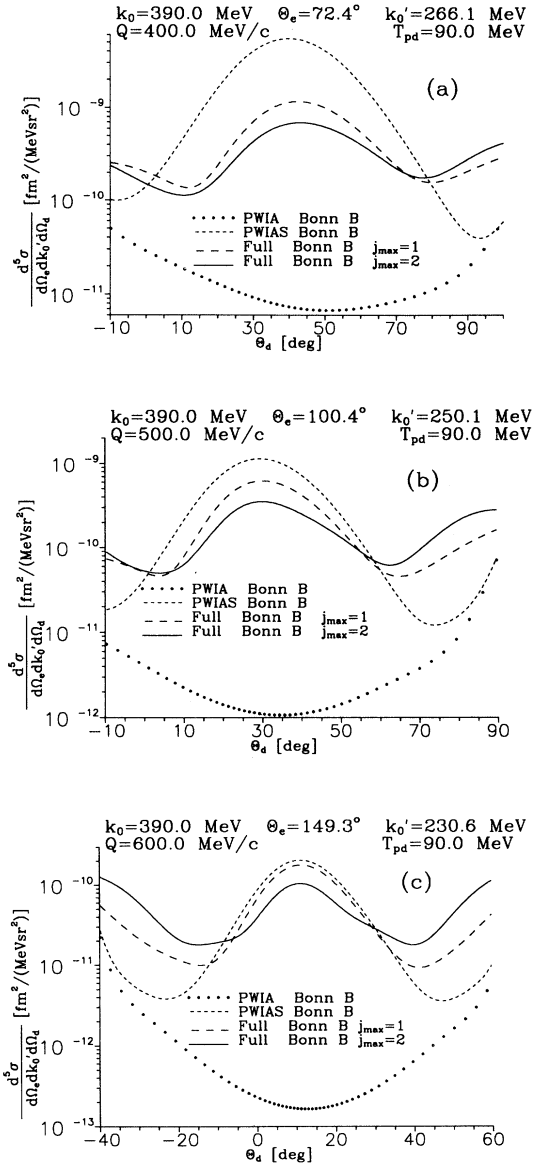

FIG. 6. The deuteron knockout peak for fixed T_{pd} and increasing $|\vec{Q}|$'s. The PWIAS predictions approach the full treatment for increasing $|\vec{Q}|$'s, but FSI remains quantitatively important for the shape and height of the peak. PWIA is totally off. The $j_{\max} = 2$ NN force contributions are very significant in all three cases: $|\vec{Q}| = 400$ MeV/c (a), $|\vec{Q}| = 500$ MeV/c (b), and $|\vec{Q}| = 600$ MeV/c (c).

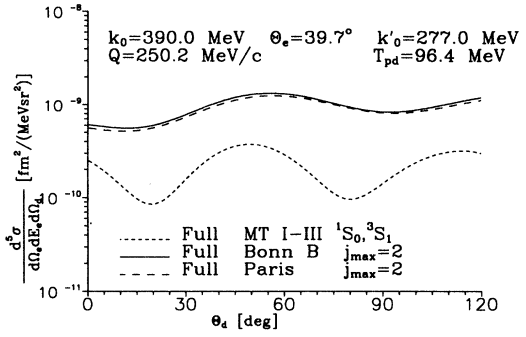

FIG. 7. The HR configuration of [26], now as a function of the deuteron scattering angle. Comparison of MT I-III, Bonn B, and Paris predictions taking FSI fully into account.

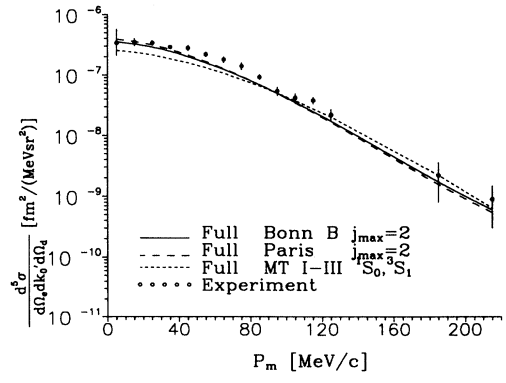

FIG. 8. Data [26], now as a function of missing momentum P_m and emphasizing deuteron knockout are compared to the Paris, Bonn B, and MT I-III predictions. FSI is taken fully into account.

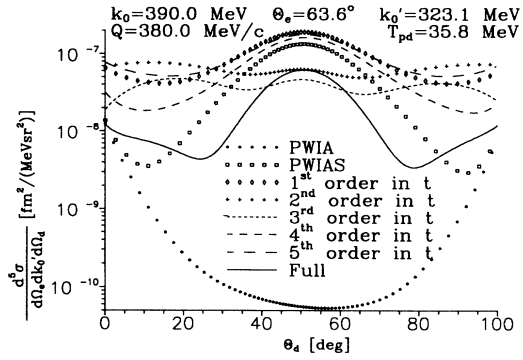

FIG. 9. The pd breakup cross section for one point in Fig. 8 ($P_m = 85$ MeV/c) as a function of the deuteron scattering angle. Comparison of PWIA, PWIAS, and partial sums of various orders in t of the multiple scattering series to the full treatment. That series is strongly diverging. The curves refer to Bonn B, $j_{\max} = 1$.

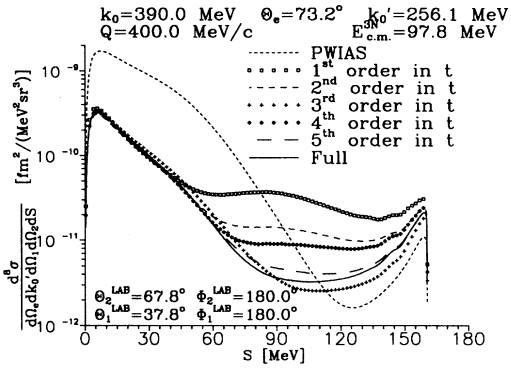

FIG. 10. The pnp breakup cross section along the arc-length S of the kinematically allowed locus in the $E_1 - E_2$ plane. One of the proton directions (particle 1) coincides with the one of the photon. Particle 2 is the neutron. Comparison of PWIAS and partial sums of the multiple scattering series in various orders of t to the full solution ($j_{\max} = 2$).

Experimental data [26] taken with $\vec{p}_d \parallel \vec{Q}$, thus emphasizing deuteron knockout are compared to the full Paris, Bonn B, and MT calculations in Fig. 8. Again the realistic NN force predictions are much closer to the data than for MT I-III. Also the $j_{\max} = 1$ results alone (not shown) are not sufficient and worse than MT I-III. As already emphasized, PWIAS (not shown) is highly insufficient and lies above the full treatment by factors between 3 and 14. In Fig. 9 we display for one point along the curve in Fig. 8 ($P_m = 85$ MeV/c corresponding to $T_{pd} = 35.8$ MeV) the angular distribution of the knocked out deuteron. One sees the expected deuteron peak. At the same time we demonstrate the strong divergence of the multiple scattering series.

B. *ppn* breakup of ^{3}He

Let us now regard the complete breakup of ^{3}He. We display only kinematically complete experiments, where in addition to the scattered electron two nucleons are detected at certain angles. Then the energies of the nucleons are kinematically correlated on a locus. We display the eight-fold differential cross section for fixed angles of the electron and the two nucleons as a function of the arclength S along that kinematical locus in the energy plane of the two detected nucleons.

First we would like to demonstrate in two examples properties of the multiple scattering series. In the first one in Fig. 10 one of the protons is ejected parallel to $\vec{Q}$ and we see a proton knockout peak at small S values. Note that here the direction of the knocked out proton is fixed and the S dependence stands for the energy distribution over the two relative motions of the three nucleons. We see that PWIAS is totally off everywhere. The curves denoted by 1st, 2nd,..., order in t are the partial sums of the multiple scattering series up to that order. While for small S values the first order in t is quite good, the higher orders are very important for larger S, where the available energy is more equally distributed over the three particles than for very small S, where the proton carries away nearly all the energy. At the larger S values only the 5th order approaches gradually the full result. A second example in Fig. 11 corresponds to a coplanar space star configuration. The three nucleons in their c.m. system have equal energies and mutual angles of 120°. In this case we show the laboratory cross section as function of the c.m. angle for particle 1 with respect to the photon direction. Here rescattering is always very important and the partial sum even of 5th order in t is not sufficient. A full solution of the $3N$ continuum Faddeev equations is required.

Due to the lack of data let us only illustrate the

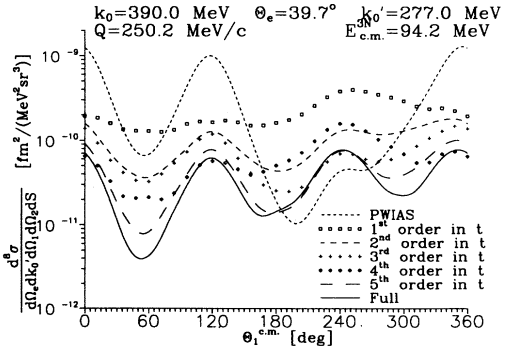

FIG. 11. The coplanar space star configuration in the pnp breakup as the function of the c.m. angle for particle 1 with respect to the photon direction. Comparison of PWIAS and partial sums of the multiple scattering series in various orders of t to the full solution ($j_{\max} = 2$).

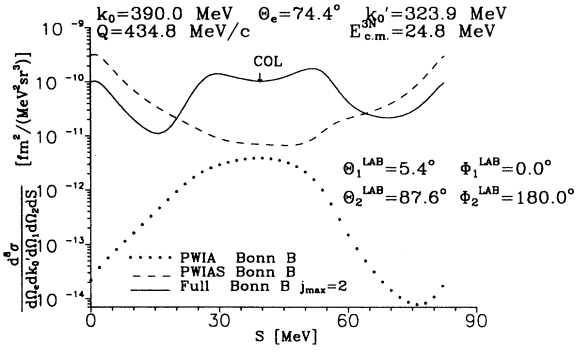

FIG. 12. The pnp breakup cross section along S for PWIA and PWIAS in comparison to a full calculation based on Bonn B ($j_{\max} = 2$). Along S the collinearity condition is valid at the point marked by an arrow.

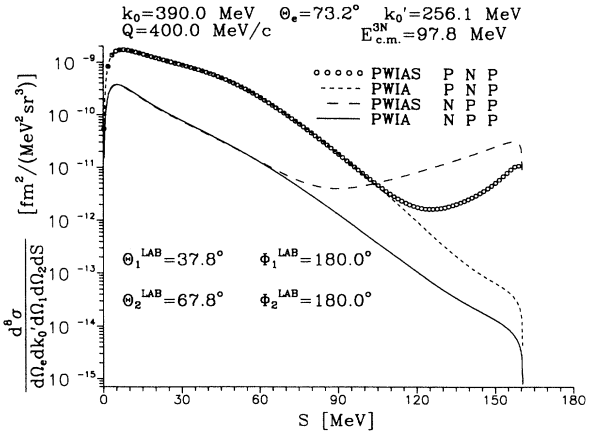

FIG. 14. Comparison of pnp and npp breakup in PWIA and PWIAS approximations. The particles 1, p, or n, have the direction of the photon and carry essentially all the available energy for small S values. At the largest S values the particle 2, proton or neutron, takes over the dominant role (for further explanations see text).

complete breakup process by two more examples, where along S one encounters specific breakup configurations known very well in the context of nd breakup studies [28]: Fig. 12 includes the condition for collinearity (in the c.m. system one nucleon is at rest) and Fig. 13 includes one FSI peak, where FSI in this context has a different meaning than elsewhere in the paper and denotes the final-state interaction between two outgoing nucleons which travel in the same direction and with the same energy. In all cases FSI is in general very important and the simple PWIAS of Eq. (14) alone is far off. All these predictions are based on the Bonn B NN force, which is included in the final state up to $j = 2$.

In view of upcoming experiments aiming at the measurement of the electric neutron form factor G_E, we regard now the configuration, where one of the final nucleon momenta, like in Fig. 10, is parallel to $\vec{Q}$. This nucleon can be either a proton or a neutron. The angle

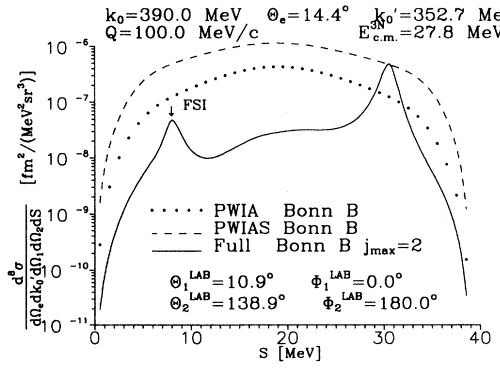

FIG. 13. The pnp breakup cross section along S for PWIA and PWIAS in comparison to a full calculation based on Bonn B ($j_{\max} = 2$). Along S two final-state interaction peaks occur. The first one (marked by an arrow) belongs to a pn pair, the second one to a pp pair. In the second case the FSI condition is not exactly fulfilled.

of a second nucleon is arbitrarily fixed. We first compare PWIA to PWIAS in Fig. 14. In the peak area for small S symmetrization plays no role and PWIA is sufficient. The cross section is overwhelmingly determined by W_T, which again results mainly from the transversal spin current. The nucleons numbered 1, 2, and 3 are chosen as pnp and npp, respectively. Since the magnetic form factor of the proton is larger in magnitude than for the neutron the proton peak height is larger, too. With increasing S the available energy is shared more equally between nucleons 1 and 2 and toward the largest S-values particle 2 takes over most of the energy. This is shown in Fig. 15. In this case the part going with P in Eq. (14) takes over the role of the first one and PWIAS separates from PWIA. Since for the sequence pnp the second nucleon is a neutron and for npp a proton the curve for pnp is lower than for npp. This is due to the different

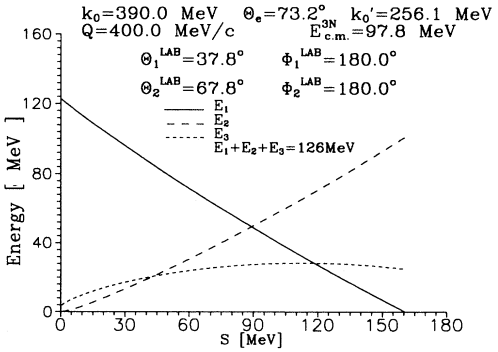

FIG. 15. The distribution of energies E_1, E_2, and E_3 along S.

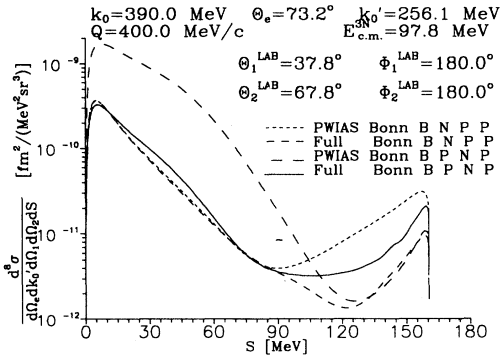

FIG. 16. Comparison of pnp and npp breakup in PWIAS to the full treatments. Note the strong rescattering effects for nearly all S values.

magnitudes of the magnetic form factors.

Let us now switch on the full final-state interaction. The effects of FSI are dramatic for nearly all S values. This is shown in Fig. 16. In a forthcoming paper we shall investigate the question of FSI further by looking into incomplete conditions, where only the electron and one knocked out nucleon is detected.

IV. SUMMARY AND OUTLOOK

We demonstrated that the final-state interaction between the three nucleons in electron induced pd and ppn ^{3}He breakup can be treated fully by solving Faddeev-like integral equations. Any realistic NN force can be used. As an example we employed the Bonn B and Paris potentials. For deuteron knockout we found good agreement to some NIKHEF data, though only the most simple nonrelativistic single nucleon current operator has been used. Thereby it was important to use realistic NN forces in all relevant partial wave states beyond $l = 0$. Data which completely map out the angular distribution of the ejected proton and especially of the deuteron in their respective peak areas would be very useful to test the rescattering processes and the current operator. The important role of the FSI is illustrated also for the breakup in some examples. The important step forward achieved in the present work is, that the role of the FSI can be checked theoretically, at least under all kinematical conditions, where relativity plays a minor role. More work and applications thereof are in progress. This also opens the door to analyze the existing data for photodisintegration of ^{3}He, pd capture reactions, and inclusive scattering on ^{3}He taking FSI fully into account. For pd capture reactions and inclusive scattering equally precise studies are already being pursued as has been mentioned in the Introduction. Especially, the renewed study of FSI corrections for y scaling will be interesting and will support or modify the results gained up to now for momentum distributions of nucleons in light nuclei. Having all the nuclear matrix elements N^μ including FSI at ones disposal, predictions will also be possible for the exciting issues of reactions with polarized electrons and ^{3}He (^{3}H) targets. Steps in those directions are being done presently.

ACKNOWLEDGMENTS

This work was supported financially by the Deutsche Forschungsgemeinschaft (H.K.) and by the Science and Technology Cooperation Germany-Poland under Grant No. X081.91. The numerical calculations were performed on the NEC SX3 of the Unversität Köln, the NEC SX3 of the Swiss Scientific Computing Center in Manno and the CRAY Y-MP of the Höchstleistungsrechenzentrum in Jülich.

[1] D. R. Lehman, Phys. Rev. Lett. **23**, 1339 (1969); Phys. Rev. C **3**, 1827 (1971).
[2] I. M. Barbour and A. C. Phillips, Phys. Rev. Lett. **19**, 1388 (1967); Phys. Rev. C **1**, 165 (1970).
[3] B. F. Gibson and D. R. Lehman, Phys. Rev. C **11**, 29 (1975); **13**, 477 (1976).
[4] D. R. Lehman, F. Prats, and B. F. Gibson, Phys. Rev. C **19**, 310 (1979).
[5] C. R. Heimbach, D. R. Lehman, and J. S. O'Connell, Phys. Lett. **66B**, 1 (1977); Phys. Rev. C **16**, 2135 (1977).
[6] E. van Meijgaard and J. A. Tjon, Phys. Rev. C **42**, 74 (1990); **42**, 96 (1990); **45**, 1463 (1992).
[7] J. Jourdan *et al.*, Nucl. Phys. **A453**, 220 (1986).
[8] S. Ishikawa and T. Sasakawa, Phys. Rev. C **45**, R1428 (1992).
[9] A. C. Fonseca and D. R. Lehman, Phys. Lett. B **267**, 159 (1991); Few-Body Systems Suppl. **6**, 279 (1992); Phys. Rev. C **48**, R503 (1993).
[10] J. L. Friar, B. F. Gibson, and G. L. Payne, Phys. Lett. B **251**, 11 (1990).
[11] R. Schiavilla and V. G. Pandharipande, Phys. Rev. C **36**, 2221 (1987); R. Schiavilla, Phys. Lett. B **218**, 1 (1985).
[12] J. Carlson and R. Schiavilla, Phys. Rev. Lett. **68**, 3682 (1992); Phys. Rev. C **49**, R2880 (1994).
[13] V. D. Efros, W. Leidemann, and G. Orlandini, Few-Body System **14**, 15 (1993).
[14] V. D. Efros, W. Leidemann, and G. Orlandini, Phys. Lett. B **338**, 130 (1994).
[15] S. Ishikawa, H. Kamada, W. Glöckle, J. Golak, and H. Witała, Nuovo Cimento A **107**, 305 (1994).
[16] W. Glöckle, J. Golak, H. Kamada, S. Ishikawa, and H. Witała, in *Proceedings of Workshop on Electron-Nucleus Scattering*, EIPC, Italy, July 1993, edited by O. Benhar, A. Fabrocini, and R. Schiavilla (World Scientific, Singapore, 1994), p. 64.
[17] J. Golak, W. Glöckle, H. Kamada, H. Witała, and S. Ishikawa, Conference Handbook of the 14th European Conference on Few-Body Problems on Physics, Amsterdam 1993, p. 106, and PAN XIII, Particles and Nuclei, XIII International Conference, Perugia, Italy, edited by A. Pasolini (World Scientific, Singapore, 1994), p. 446.
[18] H. Kamada, W. Glöckle, and J. Golak, Nuovo Cimento **105A**, 1435 (1992).
[19] Taber de Forest, J. Ann. Phys. (N.Y.) **45**, 365 (1967).

[20] T. W. Donnelly, private communication.
[21] G. G. Ohlsen, Nucl. Instrum. Methods **37**, 240 (1965).
[22] W. Glöckle, *The Quantum Mechanical Few-Body Problem* (Springer Verlag, Berlin, 1983).
[23] W. Glöckle, Lecture Notes in Physics **273**, 3 (1987); H. Witała, W. Glöckle, and Th. Cornelius, Few-Body Systems **3**, 123 (1988).
[24] R. Machleidt, Advan. Nucl. Phys. **19**, 189 (1989).
[25] E. Jans, private communication.
[26] P. H. M. Keizer, Ph.D. thesis, Amsterdam 1986.
[27] H. P. Blok, private communication; Few-Body Systems Suppl. **7**, 120 (1994).
[28] W. Glöckle, H. Witała, and Th. Cornelius, Nucl. Phys. **A508**, 115c (1990).